Vortex patch dynamics

David Dritschel

University of St Andrews

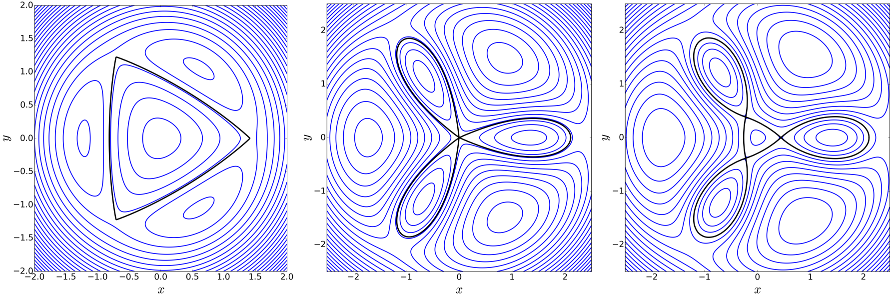

Contents

V-states for the Euler equations

The study of steadily-rotating vortex patch solutions of the 2D Euler equations

$$\frac{\mathrm{D}\omega}{\mathrm{D}t} = 0 \tag{1}$$

$$\nabla^2\psi = \omega \tag{2}$$

$$\boldsymbol{u} = \nabla^{\perp}\psi$$

began with Deem & Zabusky (1978). Before this, the ellipse was the only known steadily-rotating state.

They found m-fold symmetric generalisations ($m > 2$) of the ellipse whose limiting forms exhibit 90° corners on their boundaries (at stagnation points).

Contour Dynamics

For a vortex patch, the vorticity is *uniform* $\omega = \omega_0$ within a region $\mathcal{D}$ of $\mathbb{R}^2$ and zero otherwise. Stokes' theorem then reduces the Euler equations to

$$\frac{\mathrm{d}\boldsymbol{x}}{\mathrm{d}t} = \boldsymbol{u}(\boldsymbol{x}, t) = -\frac{\omega_0}{2\pi} \oint_{\mathcal{C}} \log(|\boldsymbol{x}' - \boldsymbol{x}|)\mathrm{d}\boldsymbol{x}' \tag{3}$$

where $\mathcal{C}$ is the bounding contour (or contours) of $\mathcal{D}$ and $\boldsymbol{x}' \in \mathcal{C}$.

- For $\boldsymbol{x} \in \mathcal{C}$, this is a closed system of equations for the evolution of $\mathcal{C}$.

These are the equations of Contour Dynamics and go back to Zabusky, Hughes & Roberts (1979) (see also Berk & Roberts 1965).

V-states are steadily-rotating or steadily-translating solutions of (3).

Vorticity interfaces: Origins of Contour Dynamics

Consider two fluid particles having the *same* vorticity, or *potential vorticity* in geophysical fluids, $\omega = \omega_0$, say.

If we exchange their positions, the distribution of $\omega(\boldsymbol{x}, t)$ is unaffected. Therefore, this has no consequence for the flow evolution.

Now consider a *vorticity interface*, a curve $\mathcal{C}$ dividing the plane into two regions of *uniform* vorticity, ω_+ and ω_-.

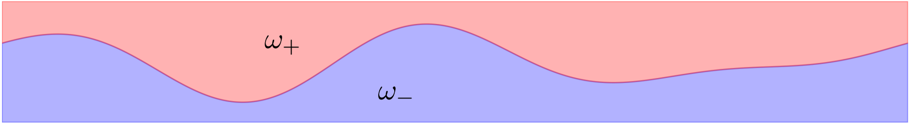

The above 'particle exchange symmetry' means that only $\mathcal{C}$ and the jump in vorticity $\Delta\omega = \omega_+ - \omega_-$ across it matter in determining the velocity field $\boldsymbol{u}$.

Vorticity interfaces

Let $\mathcal{C}$ be directed such that vorticity ω_+ lies to its left, and ω_- lies to its right. ($\mathcal{C}$ can be open or closed.)

Suppose the streamfunction ψ solves $\mathcal{L}\psi = \omega$ for some *linear operator* $\mathcal{L}$ (e.g. ∇^2), and we can write the solution in terms of a Green function $G(\boldsymbol{x}' - \boldsymbol{x})$ (e.g. $(2\pi)^{-1} \log|\boldsymbol{x}' - \boldsymbol{x}|$ when $\mathcal{L} = \nabla^2$):

$$\begin{aligned}\psi(\boldsymbol{x}, t) = &\iint \omega(\boldsymbol{x}', t) G(\boldsymbol{x}' - \boldsymbol{x}) \,\mathrm{d}x\mathrm{d}y \\ = &\,\omega_+ \iint_{\mathcal{R}_+} G(\boldsymbol{x}' - \boldsymbol{x}) \,\mathrm{d}x'\mathrm{d}y' + \\ &\,\omega_- \iint_{\mathcal{R}_-} G(\boldsymbol{x}' - \boldsymbol{x}) \,\mathrm{d}x'\mathrm{d}y'\end{aligned}$$

where $\mathcal{R}_+$ and $\mathcal{R}_-$ are the regions where $\omega = \omega_+$ and ω_-, respectively.

Vorticity interfaces

Consider the associated velocity field, $u = -\partial\psi/\partial y$ and $v = \partial\psi/\partial x$:

$$\begin{aligned}\boldsymbol{u}(\boldsymbol{x},t) = &\,\omega_+ \iint_{\mathcal{R}_+} \left(-\frac{\partial}{\partial y}, \frac{\partial}{\partial x}\right) G(\boldsymbol{x}'-\boldsymbol{x})\,\mathrm{d}x'\mathrm{d}y' + \\ &\,\omega_- \iint_{\mathcal{R}_-} \left(-\frac{\partial}{\partial y}, \frac{\partial}{\partial x}\right) G(\boldsymbol{x}'-\boldsymbol{x})\,\mathrm{d}x'\mathrm{d}y'\,.\end{aligned}$$

However, the function $G(\boldsymbol{x}'-\boldsymbol{x}) = G(\boldsymbol{x}-\boldsymbol{x}')$ is symmetric in $\boldsymbol{x}'$ and $\boldsymbol{x}$. Hence, the above can equally-well be written

$$\begin{aligned}\boldsymbol{u}(\boldsymbol{x},t) = &\,\omega_+ \iint_{\mathcal{R}_+} \left(\frac{\partial}{\partial y'}, -\frac{\partial}{\partial x'}\right) G(\boldsymbol{x}'-\boldsymbol{x})\,\mathrm{d}x'\mathrm{d}y' + \\ &\,\omega_- \iint_{\mathcal{R}_-} \left(\frac{\partial}{\partial y'}, -\frac{\partial}{\partial x'}\right) G(\boldsymbol{x}'-\boldsymbol{x})\,\mathrm{d}x'\mathrm{d}y'\,.\end{aligned}$$

Vorticity interfaces

Green's theorem (Stokes' theorem in the plane) tells us

$$\iint_{\mathcal{R}} \left(\frac{\partial Q}{\partial x'} - \frac{\partial P}{\partial y'} \right) = \int_{\mathcal{C}} P \,\mathrm{d}x' + Q \,\mathrm{d}y'$$

for (almost) any functions $P(x', y')$ and $Q(x', y')$. Here the contour $\mathcal{C}$ is traversed so that $\mathcal{R}$ is always on its left.

Therefore, taking $P = G(\boldsymbol{x}' - \boldsymbol{x})$ and $Q = 0$ for u, and taking $P = 0$ and $Q = G(\boldsymbol{x}' - \boldsymbol{x})$ for v, we have

$$\boldsymbol{u}(\boldsymbol{x}, t) = -\Delta\omega \int_{\mathcal{C}} G(\boldsymbol{x}' - \boldsymbol{x}) \,\mathrm{d}\boldsymbol{x}' \,,$$

a remarkably compact expression! The jump in vorticity $\Delta\omega$ arises because $\mathcal{C}$ is traversed in opposite directions in the two regions.

Vorticity interfaces

The *dynamics* cannot depend on fluid particles in the regions outside $\mathcal{C}$, since these particles can be exchanged arbitrarily with no effect on the velocity field $\boldsymbol{u}$.

$\Rightarrow$ Therefore, the dynamics is *entirely* dependent on $\mathcal{C}$.

We can deduce how $\mathcal{C}$ evolves by evaluating $\boldsymbol{u}$ on $\mathcal{C}$ and equating this to the material derivative of a particle *on* $\mathcal{C}$:

$$\frac{\mathrm{d}\boldsymbol{x}}{\mathrm{d}t} = -\Delta\omega \int_{\mathcal{C}} G(\boldsymbol{x}' - \boldsymbol{x})\,\mathrm{d}\boldsymbol{x}'\,.$$

This is a self-contained equation for the evolution of $\mathcal{C}$.

For 2D planar flow, this is known as 'Contour Dynamics' (Zabusky, Hughes & Roberts 1979), and in Plasma Physics, it is known as the 'Water Bag Model' (Berk & Roberts 1965).

Dritschel (1985) found co-rotating multiple-vortex states for $m = 2$ to 8 vortices, generalising the earlier work of Saffman & Szeto (1980) for $m = 2$ only.

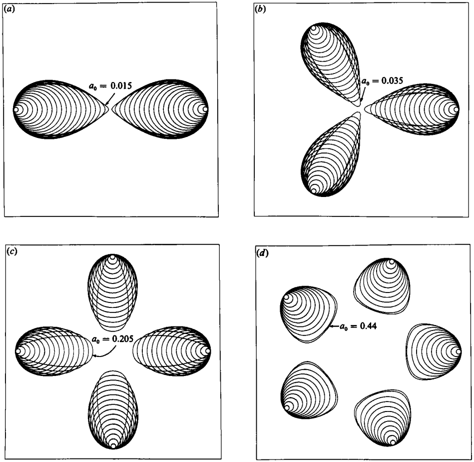

V-states for the Euler equations

Love (1893) examined the stability of the ellipse and found a sequence of instabilities, starting with an $m = 3$ mode at aspect ratio $\lambda = 1/3$, then $m = 4$ at $\lambda \approx 0.215$. etc.

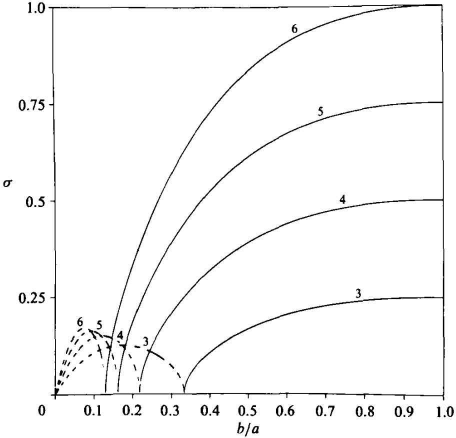

V-states for the Euler equations

Kamm (1987) and Cerretelli and Williamson (2003) found new V-states bifurcating from the elliptical solutions at the points of marginal stability.

From Luzzatto-Fegiz and Williamson (2010):

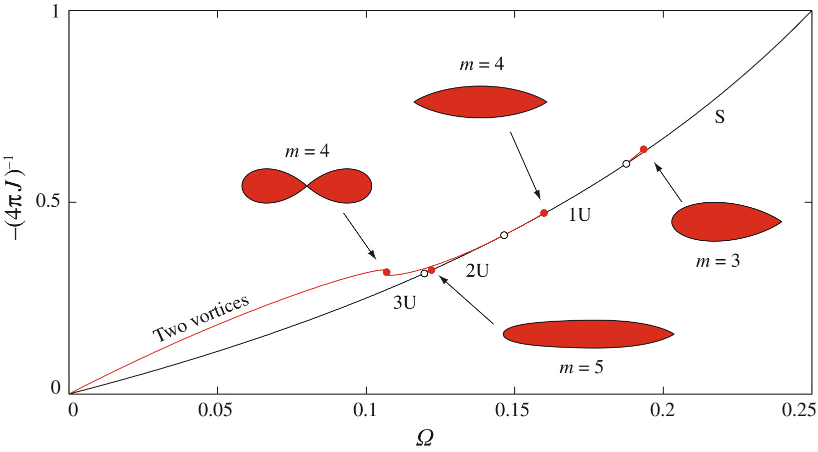

V-states for the quasi-geostrophic shallow-water equations

An important geophysical fluid dynamics generalisation is to consider the quasi-geostrophic approximation of the shallow-water equations.

This system looks similar to the 2D Euler equations except for the inversion relation between ψ and q, here the 'potential vorticity' (PV):

$$\frac{\mathrm{D}q}{\mathrm{D}t} = 0 \tag{4}$$

$$\nabla^2\psi - \gamma^2\psi = q \tag{5}$$

$$\boldsymbol{u} = \nabla^\perp\psi$$

where $\gamma = 1/L_\mathrm{D}$ and L_D is the Rossby deformation length controlling the elasticity of the free surface.

Contour Dynamics

For a vortex patch, the quasi-geostrophic equations may also be reduced to Contour Dynamics:

$$\frac{\mathrm{d}\boldsymbol{x}}{\mathrm{d}t} = \boldsymbol{u}(\boldsymbol{x}, t) = \frac{\Delta q}{2\pi} \oint_{\mathcal{C}} K_0(\gamma|\boldsymbol{x}' - \boldsymbol{x}|)\mathrm{d}\boldsymbol{x}' \qquad (6)$$

where $K_0(r)$ is the modified Bessel function of order 0.

Again, when both $\boldsymbol{x} \in \mathcal{C}$ and $\boldsymbol{x}' \in \mathcal{C}$, (6) is a closed system of equations for the evolution of $\mathcal{C}$.

V-states are steadily-rotating or steadily-translating solutions of (6).

Polvani, Zabusky and Flierl (1989) found V-states for both one and two vortices (also in one or two layers).

Two-fold symmetric V-states

Plotka and Dritschel (2010) extended the single-vortex steady states.

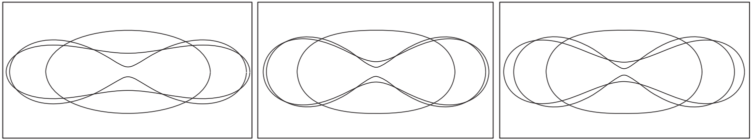

Figure 3. Selected equilibrium contour shapes for $\gamma = 0.5$ (left), 3.0 (middle) and 8.0 (right). In each frame, we show the equilibrium contours for $\lambda = 0.5$, for the aspect ratio λ_c at marginal stability, and for the smallest aspect ratio attainable λ_f. The plot window is the rectangle $|x| \le 2.2$, $|y| \lesssim 1.18$.

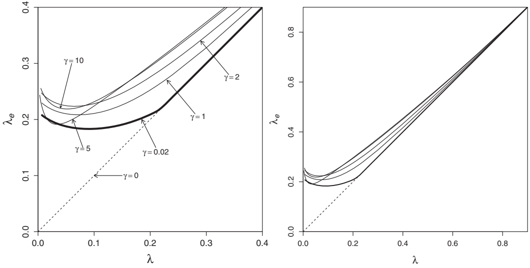

Figure 4. Comparison of the aspect ratio λ and the elliptical aspect ratio λ_e, obtained from the second spatial moments, $\int\int x^2\,\mathrm{d}x\,\mathrm{d}y$ and $\int\int y^2\,\mathrm{d}x\,\mathrm{d}y$ of the vortex patch. The equilibrium families $\gamma = 1$, 2, 5 and 10 are shown by thin lines, the family $\gamma = 0.02$ by a bold line and the barotropic Kirchhoff family $\gamma = 0$ by the dashed line. The curve for $\gamma = 10$ displays the most distortion for small λ. On the left, we see a zoom of the figure on the right.

Two-fold symmetric V-states

Plotka and Dritschel (2010) observed a continuous variation in the steady states from a near elliptical form to a dumbbell shape, even for $\gamma \ll 1$.

One might expect steady states near the Euler ellipses for smaller aspect ratio, *but none were found*.

We (Dritschel, Hmidi & Renault, *Arch. Rat. Mech. Anal.* **231(3)**, 2019) suspected that these steady states might exist but they are inaccessible from the circular state — i.e. they no longer lie on the same solution branch.

To access this distinct branch, it was necessary to develop a more sophisticated method to compute steady states.

Two-fold symmetric V-states: numerical method

The method uses a Newton iteration of the fully linearised equations about a guess for the steady state.

The linearisation itself makes use of the 'travel-time coordinate' $\vartheta = \Omega_p t$ formulated in Dritschel (1995), and first implemented by Luzzatto-Fegiz and Williamson (2010) for computing steady states.

Ω_p is the particle rotation frequency.

A correction for the vortex boundary shape (x, y) is found using

$$x^{\text{new}} = x + \frac{\eta y_\vartheta}{x_\vartheta^2 + y_\vartheta^2} \quad , \quad y^{\text{new}} = y - \frac{\eta x_\vartheta}{x_\vartheta^2 + y_\vartheta^2}$$

— this is a normal perturbation to the previous boundary shape. Note: η has units of area.

Two-fold symmetric V-states: numerical method

The quantity η is determined from

$$\Omega_{\mathrm{p}}\eta(\vartheta) + \int_0^{2\pi} \eta(\vartheta')G(|\boldsymbol{x}(\vartheta') - \boldsymbol{x}(\vartheta)|)\mathrm{d}\vartheta' = C - \psi(\vartheta) + \frac{1}{2}\Omega(x^2 + y^2)$$

where

- $\Omega_{\mathrm{p}} = 2\pi / \oint ds/|\boldsymbol{u}|$ is the particle rotation frequency around the vortex boundary,
- Δq $(= 1)$ is the jump in potential vorticity crossing into the vortex,
- $G(r) = -(2\pi)^{-1}K_0(\gamma r)$ is the Green function for the Helmholtz inversion operator,
- C is an unimportant constant,
- $\psi(\vartheta)$ is the streamfunction on the vortex boundary from the previous guess, and
- Ω is the specified equilibrium rotation rate.

- Optionally, we can specify the vortex angular impulse

$$J = \iint (x^2+y^2)q(x,y)\mathrm{d}x\mathrm{d}y = \frac{\Delta q}{4}\oint_{\mathcal{C}}(x^2+y^2)(x\mathrm{d}y - y\mathrm{d}x)$$

and determine Ω.

In practice, we add another equation, a linearisation of the above,

$$\Delta q \int_0^{2\pi} \eta(\vartheta)[x^2(\vartheta)+y^2(\vartheta)]\,\mathrm{d}\vartheta = J - \bar{J}$$

where $\bar{J}$ is the angular impulse of the previous guess.

This enables us to determine a correction Ω' to the rotation rate of the previous guess.

Two-fold symmetric V-states: numerical method

Numerically, integration is carried out by two-point Gaussian quadrature taking care to remove and exactly evaluate the logarithmic singularity in G.

800 points, approximately equally spaced in ϑ, are used to represent the vortex boundary.

The perturbation function η is expanded as a truncated, symmetric Fourier series:

$$\eta(\vartheta) = \sum_{n=1}^{N} a_n \cos(2n\vartheta)$$

The resulting linear system is solved for the coefficients a_n (and Ω') via an $N \times N$ matrix (or an $(N+1) \times (N+1)$ matrix). Here, we take $N = 32$.

An extra constant a_0 is added to η to ensure area conservation.

Two-fold symmetric V-states: results

As suspected, at any finite γ, a disconnected branch of solutions arises near the $m = 4$ margin of stability for the Euler ellipses ($\gamma = 0$).

$\underline{\gamma = 0.01}$

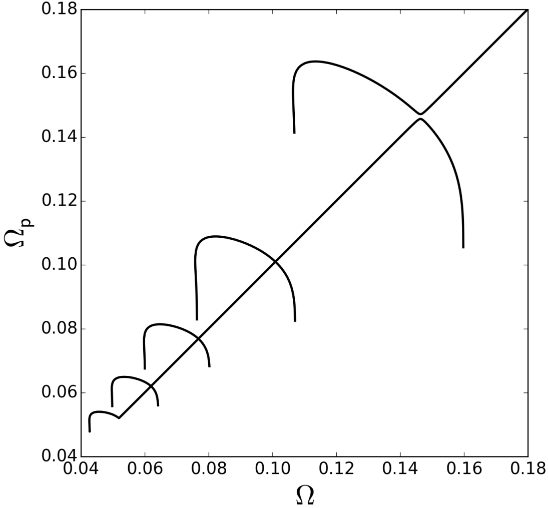

Two-fold symmetric V-states: results

However, the angular impulse J is not a particularly good statistic to see this.

$\underline{\gamma = 0.01}$

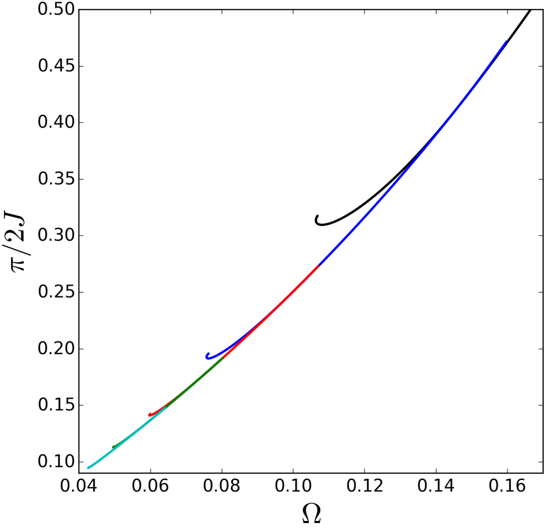

Limiting vortex shapes and ψ for $\gamma = 0.01$

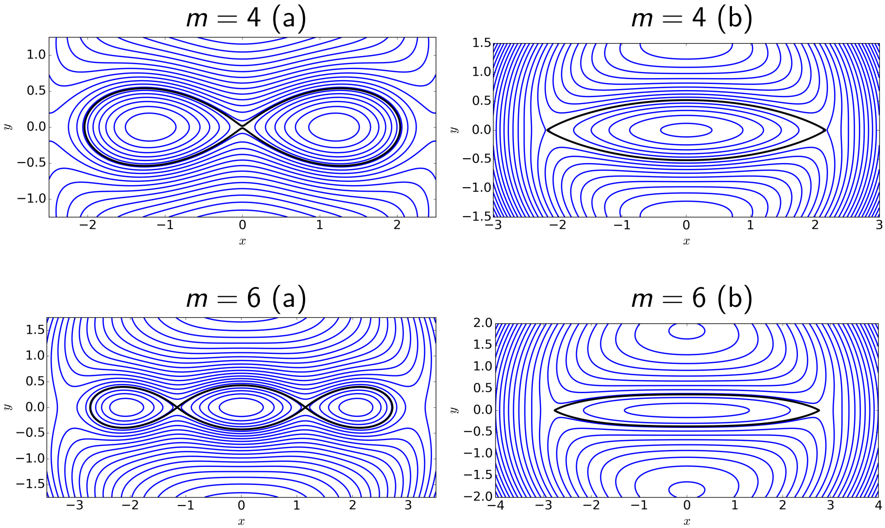

Limiting vortex shapes and ψ for $\gamma = 0.01$

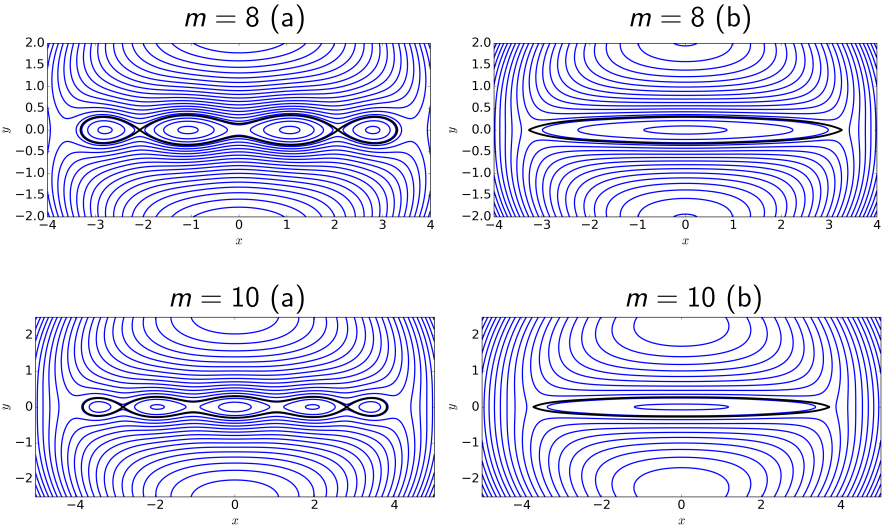

Larger γ

At larger γ, a second disconnected branch of solutions arises near the $m = 6$ margin of stability for the Euler ellipses! Are all disconnected?

$\underline{\gamma = 0.1}$

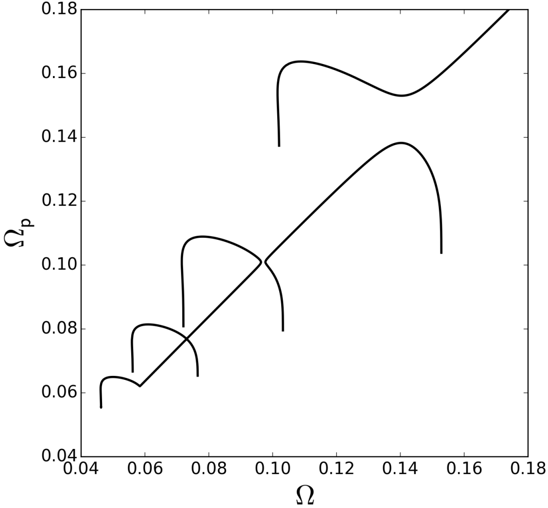

Larger γ

It gets even more strange as γ increases further. Here $\gamma = 1$.

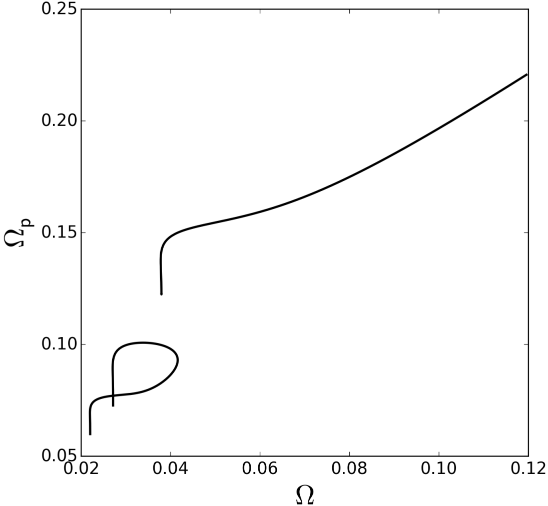

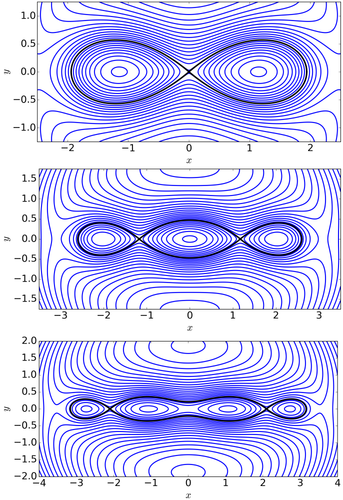

Three-fold symmetric V-states

For the three-fold symmetric V-states, originally found for the Euler equations by Deem & Zabusky (1978), we (Dritschel, Hmidi & Renault, 2019) also suspected that there is another, separated branch of steady states.

This was discovered first at large γ, then traced all the way back to $\gamma = 0$.

We employed the same numerical method as before, optionally varying the vortex rotation rate Ω or the vortex angular impulse J.

We had to interchangeably vary Ω or J to trace the solution branches around many folds and spirals.

Three-fold symmetric V-states: equilibria

Multiple turning points occur: the branch spirals endless times as $\Omega_p \to 0$.

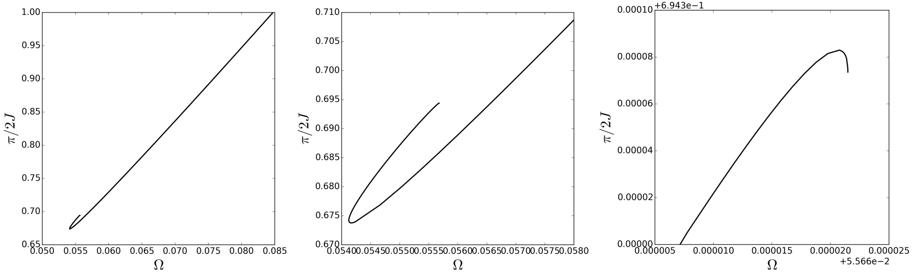

Here, the main solution branch for $\gamma = 2$ is shown.

Three-fold symmetric V-states: bifurcation

$\gamma = 3.5$
$\gamma = 3.6$

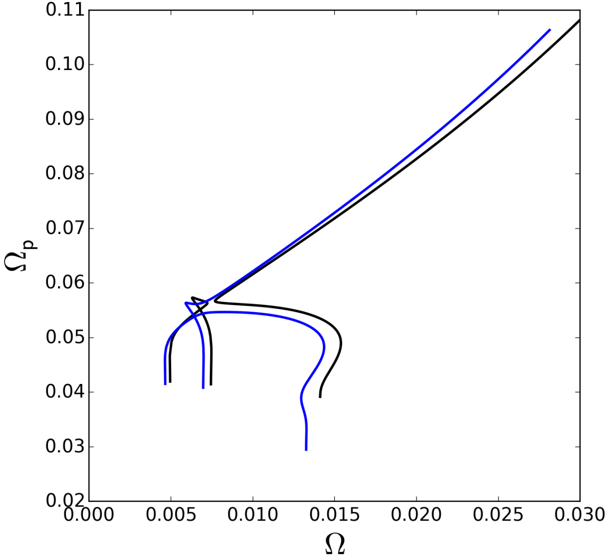

Limiting states for $\gamma = 3.6$ (Ω increases from left to right)

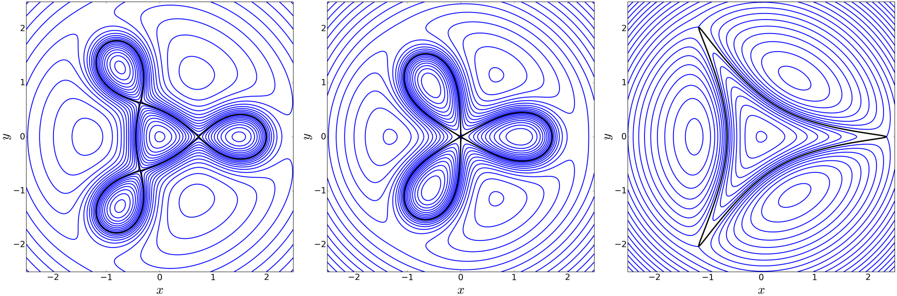

• For smaller γ, the limiting state is triangular, as on the right. Then the three and four-vortex states are on a separate branch of solutions.

• For larger γ, the limiting state is the three-vortex state, as in the middle. Then the triangular and four-vortex states are on a separate branch of solutions.

Three-fold symmetric V-states: Euler limit

$\underline{\gamma = 0}$

blue: stable
red: unstable

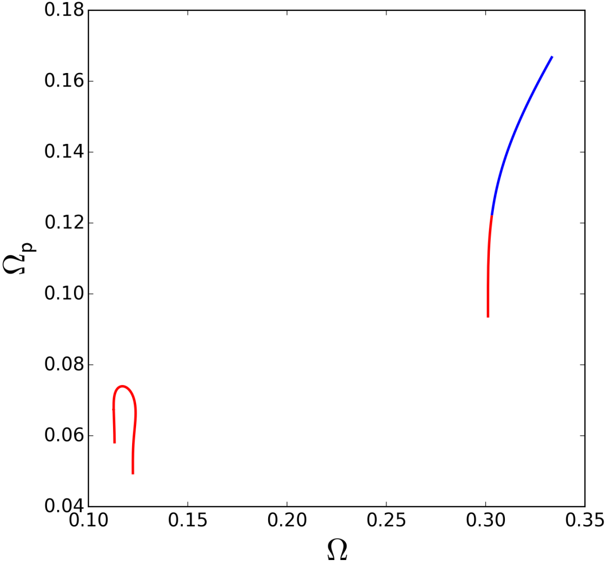

Limiting states for $\gamma = 0$ (Ω increases from left to right)

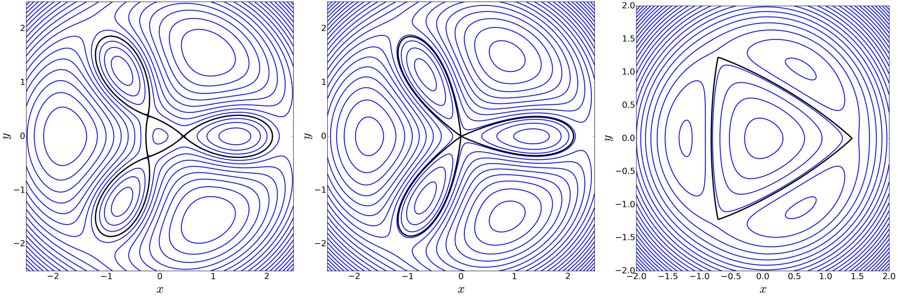

new Dritschel (1985) Deem & Zabusky (1978)

Three-fold symmetric V-states: Summary of all states

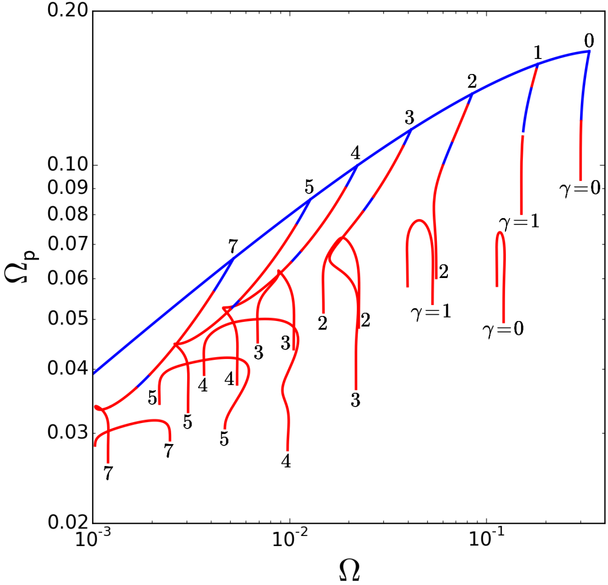

Three-fold symmetric V-states: Evolution for $\gamma = 0$

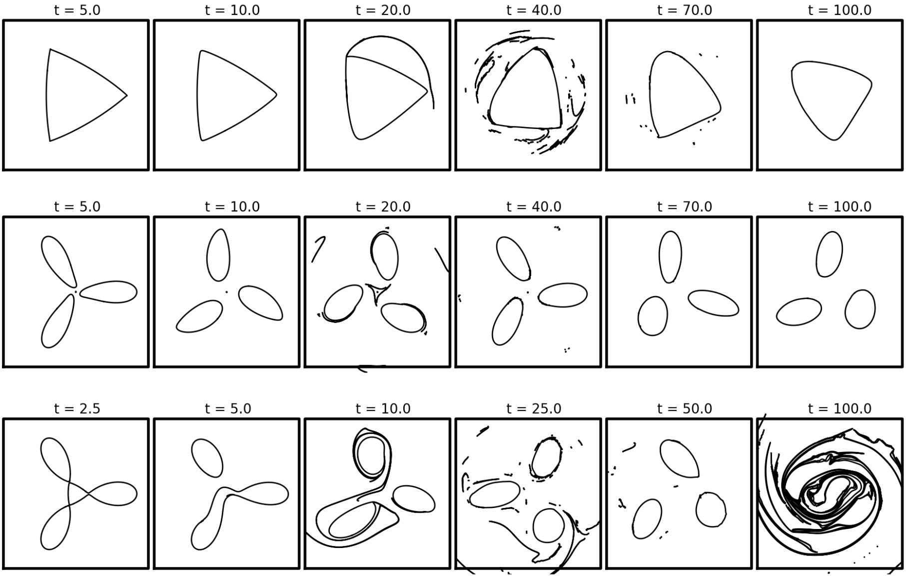

Three-fold symmetric V-states: Evolution for $\gamma = 3.6$

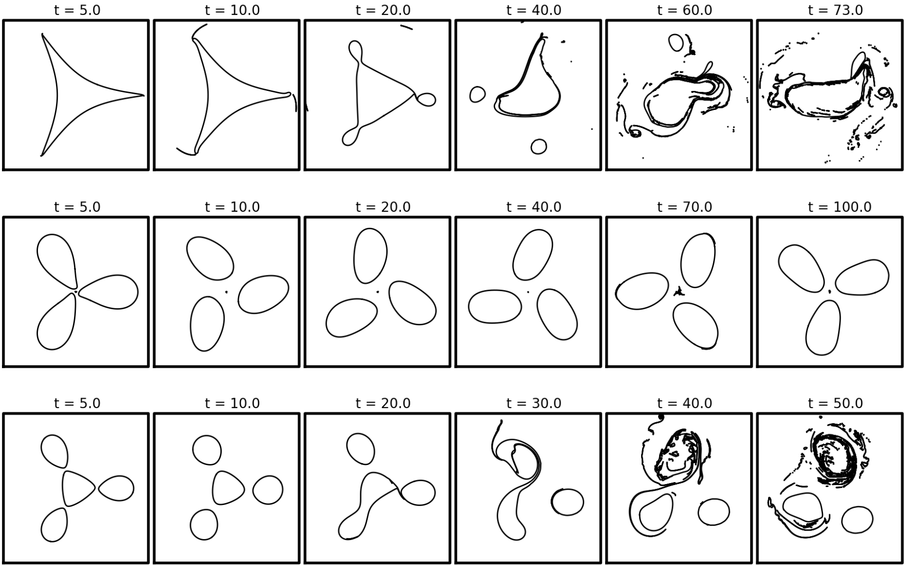

Like-signed, unequal vortices: Co-rotating equilibria

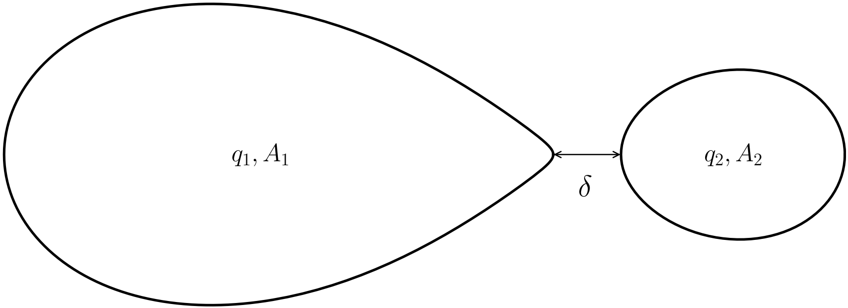

Key parameters:

(1) Area ratio A_2/A_1,
(2) PV ratio q_2/q_1,
(3) the inner gap δ, and
(4) the inverse Rossby deformation length γ.

Like-signed, unequal vortices: Co-rotating equilibria

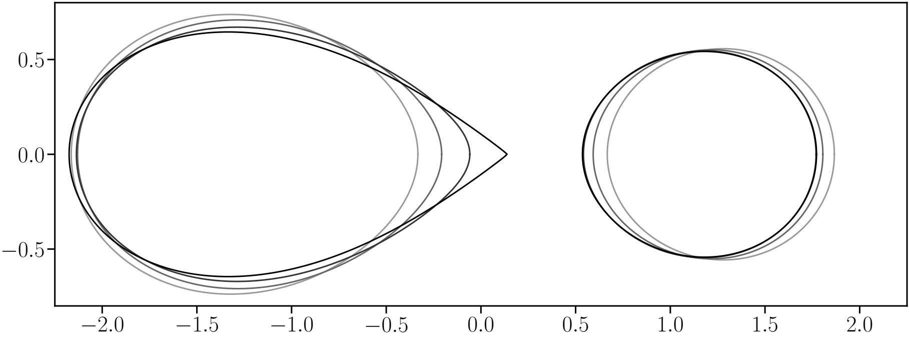

V-states having $A_2/A_1 = 0.5$, $q_2/q_1 = 2$ and $\gamma = 1$.
Shown are 4 different values of the gap: $\delta = 1$ (lightest grey), $\delta = 0.8$ (light grey), $\delta = 0.6$ (dark grey) and $\delta = 0.4$ (black).

From Jalali & Dritschel, *GAFD* 2018.

Linear stability of vortex patch equilibria: The method

To *maximally* simplify the analysis, the boundary $\mathcal{C}$ of each equilibrium vortex patch is parametrised by the ***travel-time coordinate*** ϑ:

$$\boldsymbol{x} = (\bar{x}(\vartheta), \bar{y}(\vartheta))$$

in the frame of reference rotating (or translating) with the equilibrium.

The travel-time coordinate $\vartheta = \Omega_p t = 2\pi t / T$ where

$$T = \oint_{\mathcal{C}} \frac{ds}{\bar{u}_{\|}}$$

is the orbital period, s is arc length, and $u_{\|}$ is the tangential velocity along $\mathcal{C}$. Similarly,

$$t(s) = \int_0^s \frac{ds}{\bar{u}_{\|}}$$

given some chosen starting point at $s = 0$.

Linear stability of vortex patch equilibria: The method

The optimal way to express disturbances is through

$$x(\vartheta,t)=\bar{x}+\frac{\eta\bar{y}_\vartheta}{\bar{x}_\vartheta^2+\bar{y}_\vartheta^2}\quad,\quad y(\vartheta,t)=\bar{y}-\frac{\eta\bar{x}_\vartheta}{\bar{x}_\vartheta^2+\bar{y}_\vartheta^2}$$

where a ϑ subscript denotes differentiation, and $\eta(\vartheta,t)$ is the displacement function (and has units of area) — Dritschel, *JFM* **293**, 1995, Appendix B.

Then, expanding the Contour Dynamics equations to first order in η,

$$\frac{\partial\eta}{\partial t}+\Omega_p\frac{\partial\eta}{\partial\vartheta}=\frac{\partial F}{\partial\vartheta}$$

$$F(\vartheta,t)=-\Delta q\int_0^{2\pi}\eta(\alpha,t)G(\bar{\boldsymbol{x}}(\alpha)-\bar{\boldsymbol{x}}(\vartheta))\,\mathrm{d}\alpha \tag{7}$$

where $G(\boldsymbol{x}'-\boldsymbol{x})$ is the Green function of the equation $\mathcal{L}\psi=q$ relating streamfunction ψ to PV (or vorticity) q. The PV jump across $\mathcal{C}$ is Δq.

Linear stability of vortex patch equilibria: The method

The Green function for various flow models:

- Planar 2D (Euler), $\nabla^2\psi = \omega$

  $\Rightarrow \; G(\boldsymbol{r}) = (2\pi)^{-1}\log(|\boldsymbol{r}|)$

- QG shallow-water, $\nabla^2\psi - \gamma^2\psi = q$

  $\Rightarrow \; G(\boldsymbol{r}) = -(2\pi)^{-1}K_0(\gamma|\boldsymbol{r}|)$

- 2D (Euler) on a cylinder (or x periodic), $\nabla^2\psi = \omega$

  $\Rightarrow \; G(x'-x, y'-y) = (4\pi)^{-1}\log(\cosh(y'-y) - \cos(x'-x))$

- 3D QG, $\nabla^2_{3D}\psi = q$

  $\Rightarrow \; G(\boldsymbol{r}) = -(4\pi|\boldsymbol{r}|)^{-1}$.

Linear stability of vortex patch equilibria: The method

The method trivially generalises to any number of contours $\mathcal{C}_k$, $k = 1, \ldots, n$ with PV jumps Δq_k:

$$\frac{\partial \eta_k}{\partial t} + \Omega_{p,k} \frac{\partial \eta_k}{\partial \vartheta_k} = \frac{\partial F_k}{\partial \vartheta_k}$$

$$F_k(\vartheta_k, t) = -\sum_{j=1}^{n} \Delta q_j \int_0^{2\pi} \eta_j(\vartheta_j', t) G(\bar{\boldsymbol{x}}_j(\vartheta_j') - \bar{\boldsymbol{x}}_k(\vartheta_k)) \, \mathrm{d}\vartheta_j' \,. \qquad (8)$$

Remarkably, it does *not* explicitly depend on the rotation rate Ω or translation rate (U, V) of the equilibrium configuration.

Numerically, η_k is expanded as a truncated Fourier series in ϑ_k:

$$\eta_k(\vartheta_k, t) = e^{-\mathrm{i}\sigma t} \sum_{m=1}^{M} A_m \cos m\vartheta + B_m \sin m\vartheta$$

where σ is determined as an eigenvalue.

Linear stability: results

Real and imaginary parts of σ, respectively frequency and growth rate, for V-states having $A_2/A_1 = 0.5$, $q_2/q_1 = 2$ and $\gamma = 1$.

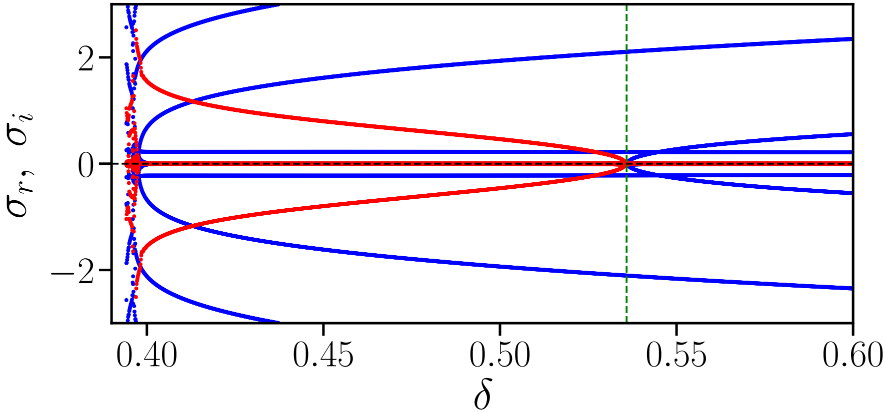

- Instability occurs below a critical gap, $\delta = \delta_c \approx 0.536$.

Minimum gap to ensure linear stability

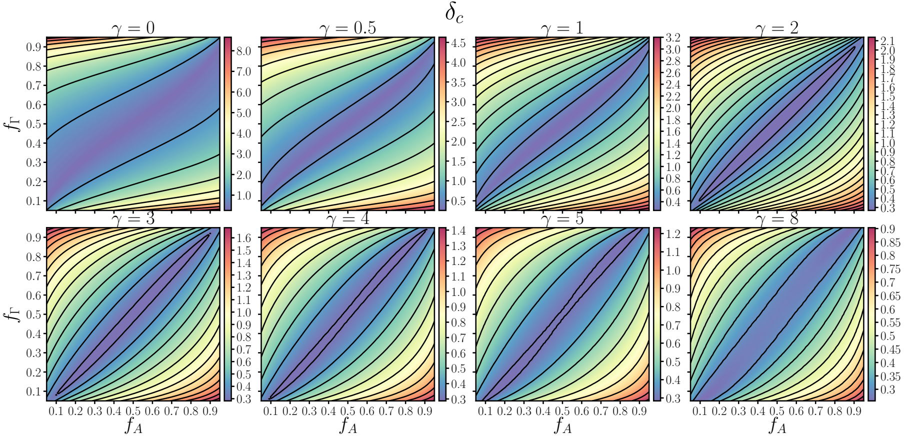

Critical gap $\delta = \delta_c$ below which equilibria are unstable, plotted versus the vortex area fraction $f_A = A_2/(A_1 + A_2)$ and the vortex circulation fraction $f_\Gamma = \Gamma_2/(\Gamma_1 + \Gamma_2)$, for several values of γ.

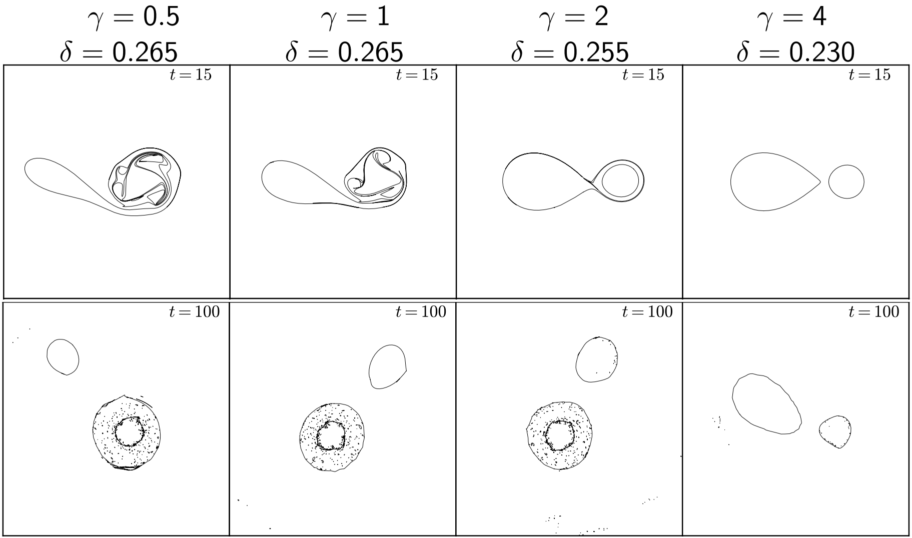

Here, $A_2/A_1 = 0.25$ and $q_2/q_1 = 2$. [movies]

Opposite-signed equilibria and linear stability

$\gamma = 1$, stable
marginal & unstable

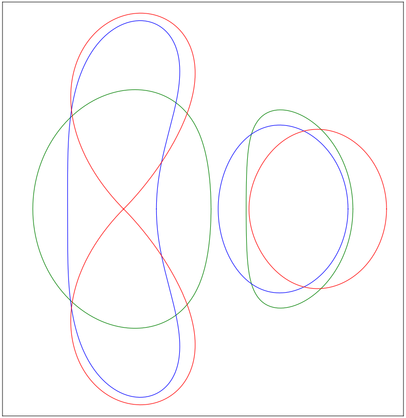

marginal stability
$\gamma = 0,\ 0.5,\ 1,\ 2,\ 4$

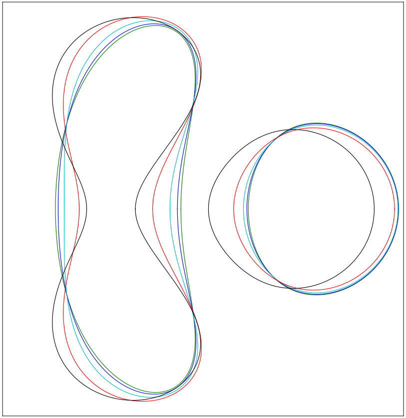

Here, $A_2/A_1 = 0.5$ and $q_2/q_1 = -0.5$. (Jalali & Dritschel, *GAFD* 2020).

$\gamma = 1$, stable
marginal & unstable

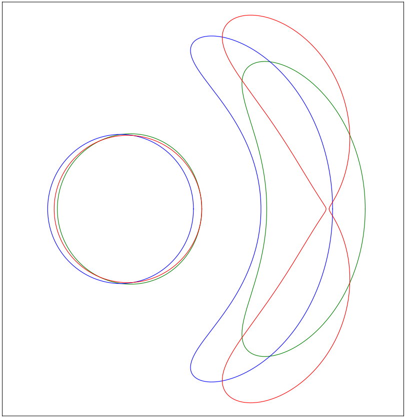

marginal stability
$\gamma = 0,\ 0.5,\ 1,\ 2,\ 4$

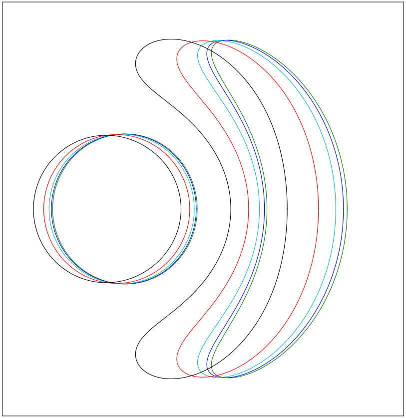

Here, $A_2/A_1 = 1.5$ and $q_2/q_1 = -4/21$. (Jalali & Dritschel, *GAFD* 2020).

Nonlinear evolution

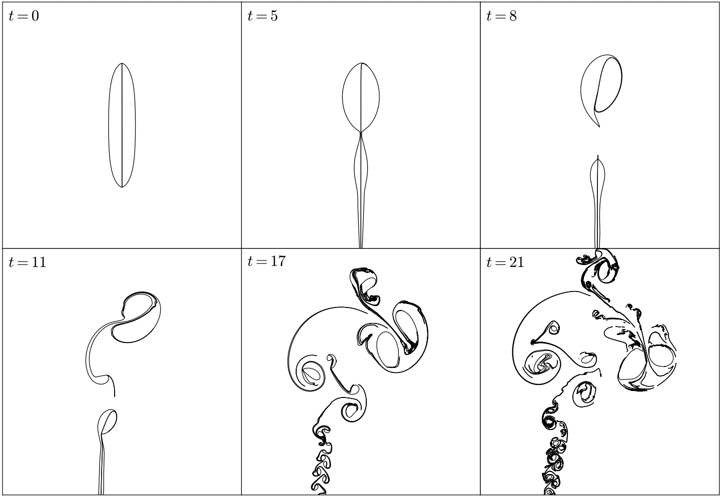

- This is a near-limiting translating V-state with $\gamma = 4$. [movies]

V-states in 3D quasi-geostrophic flows: Foundations

In the three-dimensional (3D) quasi-geostrophic (QG) model, for constant Coriolis and buoyancy frequencies, f and N, the layerwise-2D flow $(u(x,y,z,t), v(x,y,z,t))$ is determined by

$$\frac{\partial^2\psi}{\partial x^2} + \frac{\partial^2\psi}{\partial y^2} + \frac{\partial^2\psi}{\partial z^2} = \nabla^2\psi = q \quad \text{and} \quad u = -\frac{\partial\psi}{\partial y} \ \ \& \ \ v = \frac{\partial\psi}{\partial x}\,,$$

where q is the QG potential vorticity (PV) and z has been s t r e t c h e d by N/f (typically $\gg 1$ in the atmosphere and oceans).

In the absence of forcing and diabatic effects, PV is *materially conserved*:

$$\frac{\mathrm{D}q}{\mathrm{D}t} = \frac{\partial q}{\partial t} + u\frac{\partial q}{\partial x} + v\frac{\partial q}{\partial y} = 0\,.$$

V-states in 3D quasi-geostrophic flows: Origins in 2D

- Kirchhoff (1876) discovered an *exact*, steadily-rotating elliptical patch of uniform vorticity $\omega = \omega_0$ in an ideal 2D fluid.

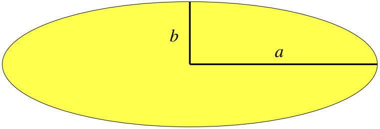

$$\Omega = \frac{\omega_0 \lambda}{(1+\lambda)^2} \quad \text{where} \quad \lambda = \frac{b}{a}$$

- Moore & Saffman (1971) then Kida (1981) generalised this solution to include a background straining and rotating flow — shape and orientation generally time dependent.

- Dritschel (1990) examined linear and nonlinear stability — rich!

- In the 3D Quasi-Geostrophic model of geophysical flows, Zhmur & Shchepetkin (1991) and Meacham (1992) discovered the ellipsoidal analogues of Kirchhoff's elliptical vortex.
- An ellipsoid $x^2/a^2 + y^2/b^2 + z^2/c^2 \le 1$ of uniform potential vorticity $q = q_0$ rotates steadily at a rate $\Omega = q_0 F(\lambda, \mu)$ where $\lambda = b/a$ and $\mu = c/\sqrt{ab}$. These solutions stem from work by Maclaurin (1742) and Laplace (1784).
- Dritschel, Scott & Reinaud (2005) examined linear and nonlinear stability.

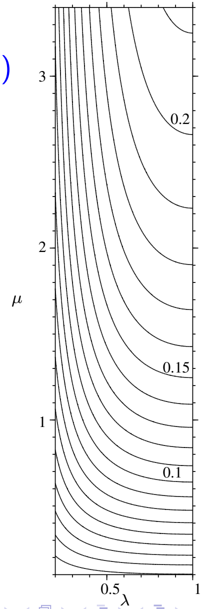

An historical survey

- Miyazaki, Ueno & Shimonishi (1999) found steadily-rotating tilted spheroidal vortices and investigated their linear stability.
- Meacham, Pankratov, Shchepetkin & Zhmur (1994), Hashimoto, Shimonishi & Miyazaki (1999) and McKiver & Dritschel (2003) added a background straining flow (leads to time-dependent shape variations).
- McKiver & Dritschel (2006) examined the stability of all steady vortices in a general straining flow.
- Dritschel, McKiver & Reinaud (2004) developed the Ellipsoidal Model.
- etc...!

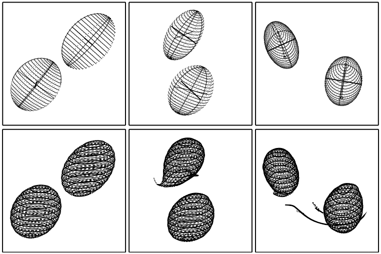

The 3D QG model has a Contour Dynamics formulation in $\mathbb{R}^3$.

◇ ◇ ◇ ◇ ◇ ◇ ◇ ◇ ◇ ◇ ◇ ◇ ◇ ◇ ◇ ◇ ◇ ◇

Consider a volume V bounded by contours $\mathcal{C}(z)$ at each height z. Let $q = \Delta q$ (uniform PV) inside V and $q = 0$ outside.

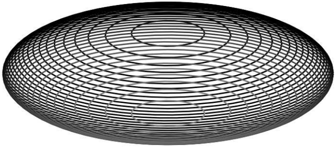

Using the Green function $-1/(4\pi|\boldsymbol{x}' - \boldsymbol{x}|)$ for Laplace's operator in 3D, we have

$$(u(\boldsymbol{x},t), v(\boldsymbol{x},t)) = \frac{\Delta q}{4\pi} \int \mathrm{d}z' \oint_{\mathcal{C}(z')} \frac{(\mathrm{d}x', \mathrm{d}y')}{|\boldsymbol{x}' - \boldsymbol{x}|}$$

where $\boldsymbol{x} = (x, y, z)$ (Dritschel, *JFM* **455** (2002), Appendix A).

This follows because the Green function is symmetric in $\boldsymbol{x}$ and $\boldsymbol{x}'$.

Contour Dynamics

In the numerical algorithm, the total height spanned by V is discretized into n layers of equal thickness, Δz. Over each layer, $(x, y) \in \mathcal{C}$ is taken to be independent of z.

Then, the z integral over each layer can be performed exactly. Evaluating it in the middle of each layer, at $z = \bar{z}_j$ ($j = 1, , ..., n$) leads to

$$\left(\frac{\mathrm{d}x_j}{\mathrm{d}t}, \frac{\mathrm{d}y_j}{\mathrm{d}t}\right) = (u_j, v_j) = \frac{\Delta q}{4\pi} \sum_{k=1}^{n} \oint_{\mathcal{C}_k} \left(\lambda_{jk}^{+} - \lambda_{jk}^{-}\right) (\mathrm{d}x'_k, \mathrm{d}y'_k)$$

where

$$\lambda_{jk}^{\pm} \equiv \log\left[\left(\rho^2 + \sigma^2\right)^{\frac{1}{2}} + \sigma\right], \qquad \sigma = |\bar{z}_j - \bar{z}_k| \pm \tfrac{1}{2}\Delta z$$

and $\rho^2 = (x_j - x'_k)^2 + (y_j - y'_k)^2$ — *all with $\mathcal{O}(\Delta z^2)$ error.*

Like *and* opposite-signed V-states in 3D QG

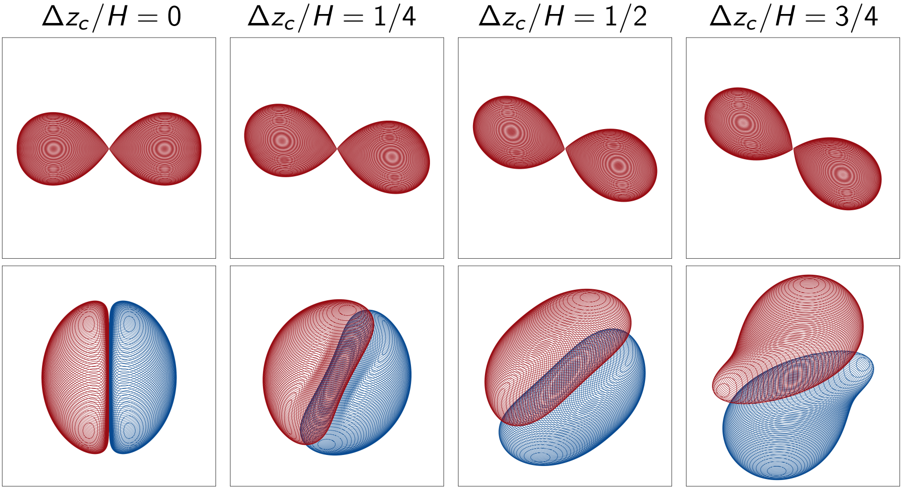

From Reinaud & Dritschel *JFM* **848** (2018) and *JFM* **971** *(2023).*

Multi-polar (like-signed) V-states in 3D QG

Top view | Side view

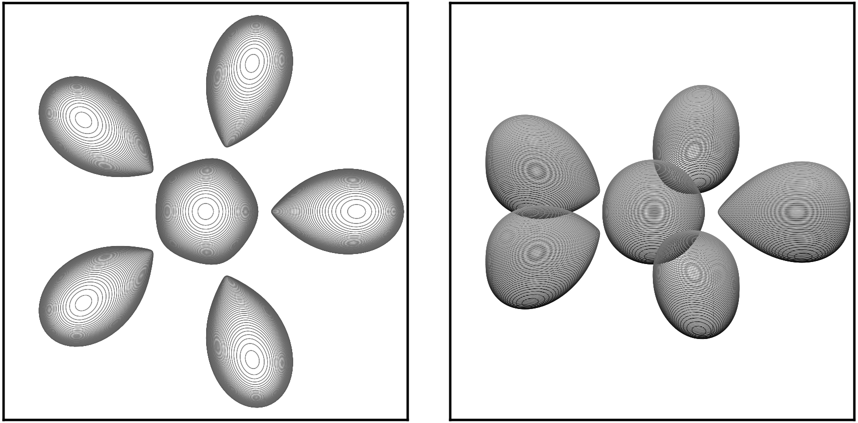

From Reinaud *AIP Advances* **12** (2022).

Multi-polar (like-signed) V-states in 3D QG

Top view

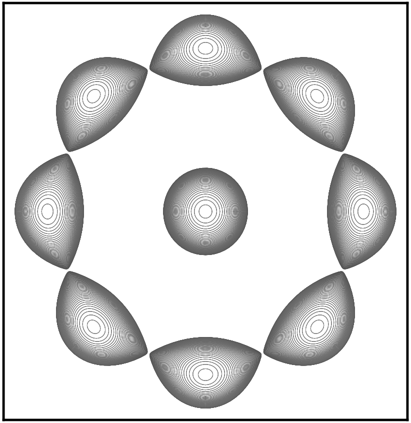

Side view

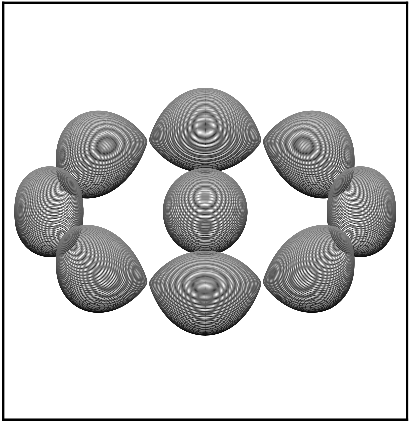

From Reinaud *AIP Advances* **12** (2022).

Nonlinear evolution

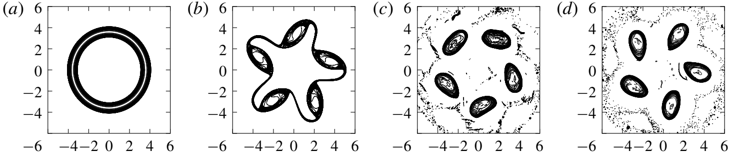

FIGURE 7. Evolution of a uniform-PV torus with $R_0/r_0 = 7.2$. Top view of the bounding contours at $t = 0,\ 26,\ 129$ and 408.

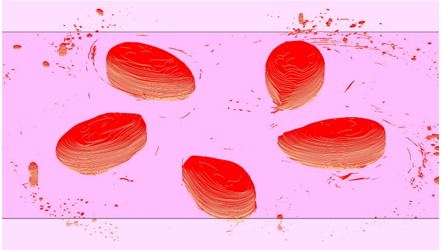

FIGURE 8. (Colour online) Orthographic view of the PV field at an angle of 60° from the vertical for the torus with $R_0/r_0 = 7.2$ at $t = 100$. The horizontal lines indicate the vertical extent of the domain of view, here $|z| \leqslant 0.5$. Flow structures seen through the lower front

Nonlinear evolution

Left: JUNO image of the south pole of Jupiter from Adriani et al, Nature **555** *(2018).*

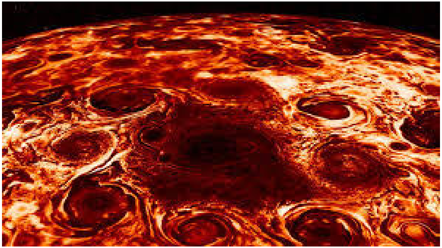

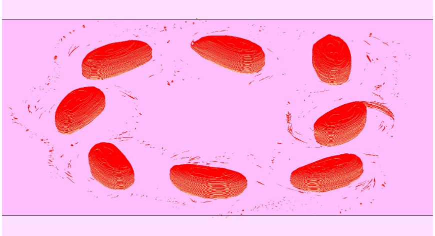

Right: Contour Surgery simulation from Reinaud & Dritschel, JFM **863** *(2019).* [movies]

Conclusions: part 1 of 2

Vortex patches in many flow models are governed by a reduced dynamical system, ‘Contour Dynamics’: *only vorticity interfaces matter.*

Such flow models include — but are not limited to — 2D planar (Euler), shallow-water quasi-geostrophic, and 3D quasi-geostrophic.

In the shallow-water quasi-geostrophic model, at finite Rossby deformation length L_{D}, the Euler elliptical branch of steady-state solutions separates near the $m = 4$ marginal stability of the Euler ellipses ($\lambda \approx 0.215$).

In fact separations appear to occur at all even higher-order bifurcations ($m = 6$, 8, 10, etc.).

A new, separated branch of solutions has been discovered for the three-fold symmetric V-states. The limiting states of this new branch and the one starting from circular states change around $\gamma = 1/L_{\mathrm{D}} = 3.5$.

There are a *plethora* of multiply-connected V-states, e.g. both like-signed and opposite-signed vortex pairs. They are stable unless sufficiently close together.

V-states of the 3D quasi-geostrophic model resemble patterns observed at the poles of the gas giant planets. In particular, patterns of 5 or 8 vortices exhibit robust stability.